lead to apparent autocatalytic kinetics for asphaltene decomposition.

Registry No. PDB, 2131-18-2; 1-tetradecene, 1120-36-1; styrene, 100-42-5; *n*-tridecane, 629-50-5; ethylbenzene, 100-41-4; toluene, 108-88-3.

Literature Cited

Badger, G. M.; Kimber, R. W. L.; Novotny, J. *Aust. J. Chem.* **1964**, *17*, 78.
Badger, G. M.; Spotswood, T. M. *J. Chem. Soc.* **1960**, 4420.
Benson, S. W. *Thermochemical Kinetics*; Wiley: New York, 1976.
Blouri, B.; Handam, F.; Herault, D. *Ind. Eng. Chem. Process Des. Dev.* **1985**, *24*, 30.
Crowne, C. W. P.; Grigulis, V. J.; Throssell, J. J. *Trans. Faraday Soc.* **1969**, *65*, 1051.
Esteban, G. L.; Kerr, J. A.; Trotman-Dickenson, A. F. *J. Chem. Soc.* **1963**, 3873.
Fabuss, B. M.; Smith, J. O.; Satterfield, C. N. In *Advances in Petroleum Chemistry and Refining*; McKetta, J. J., Jr., Ed.; Wiley: New York, 1964; Vol. 9.
Gilbert, K. E.; Gajewski, F. J. *J. Org. Chem.* **1982**, *47*, 4899.
Gould, K. A. *Fuel* **1978**, *57*, 756.
Ignasiak, T.; Bimer, J.; Samman, N.; Montgomery, D. S.; Strausz, O. P. In *Chemistry of Asphaltenes*; Bunger, J. W., Li, N. C., Eds.; Advances in Chemistry Series No. 195; American Chemical Society: Washington, DC, 1981; p 183.
Klein, M. T.; Virk, P. S. *Ind. Eng. Chem. Fundam.* **1983**, *22*, 35.
Lawson, J. R.; Klein, M. T. *Ind. Eng. Chem. Fundam.* **1985**, *24*, 203.
Leigh, C. H.; Szwarc, M. *J. Chem. Phys.* **1952**, *20*, 407.
Miller, D. B. *Ind. Eng. Chem. Prod. Res. Dev.* **1963**, *2*, 220.
Mushrush, G. W.; Hazlett, R. N. *Ind. Eng. Chem. Fundam.* **1984**, *23*, 288.
Poutsma, M. L.; Dyer, C. W. *J. Org. Chem.* **1982**, *47*, 4903.
Rebick, C. In *Thermal Hydrocarbon Chemistry*; Oblad, A. G., Davis, H. G., Eddinger, R. T., Eds.; Advances in Chemistry No. 170; American Chemical Society: Washington, DC, 1979; p 1.
Savage, P. E.; Klein, M. T.; Kukes, S. G. *Ind. Eng. Chem. Process Des. Dev.* **1985**, *24*, 1169.
Schlosberg, R. H.; Ashe, T. R.; Pancirov, R. J.; Donaldson, M. *Fuel* **1981**, *60*, 201.
Simmons, M. B.; Klein, M. T. *Ind. Eng. Chem. Fundam.* **1985**, *25*, 55.
Speight, J. G. *Fuel* **1970**, *49*, 76.
Speight, J. G.; Moschopedis, S. M. In *Chemistry of Asphaltenes*; Bunger, J. W., Li, N. C., Eds.; Advances in Chemistry Series No. 195; American Chemical Society: Washington, DC, 1981; p 1.
Suruki, T.; Itoh, M.; Takegami, Y.; Watanabe, Y. *Fuel* **1982**, *61*, 402.
Szwarc, M. *J. Chem. Phys.* **1948**, *16*, 128.
Szwarc, M. *J. Chem.* Phys. **1949**, *17*, 431.
Takegami, Y.; Watanabe, Y.; Suzuki, T.; Mitsudo, T.; Itoh, M. *Fuel* **1980**, *59*, 253.
Yen, T. F. *Energy Sources* **1974**, *1*, 447.
Yen, T. F. In *Chemistry of Asphaltenes*; Bunger, J. W., Li, N. C., Eds.; Advances in Chemistry Series No. 195; American Chemical Society: Washington, DC, 1981; p 39.

Received for review August 12, 1985
Accepted July 18, 1986

HDS Kinetic Studies on Greek Oil Residue in a Spinning Basket Reactor

Jamal M. Ammus and George P. Androutsopoulos*
Department of Chemical Engineering, National Technical University of Athens, GR 106 82 Athens, Greece

A spinning basket reactor was used to investigate the hydrodesulfurization (HDS) kinetics of Greek (Thasos) atmospheric residue. The effects of temperature (285–395 °C), pressure (30–70 bar), and particle size ($\bar{L}_p = 5.67 \times 10^{-3}$–$58.9 \times 10^{-3}$ cm) upon the intrinsic reaction rate were determined. Two commercial HDS supported catalysts (Co–Mo/γ-Al_2O_3) differing in their chemical composition and physical structure were employed. It was shown that the overall HDS reaction rate was kinetically controlled when the pulverized catalyst was rotated at a rate of 2540 rpm. Parameters defined by a general lumped kinetic equation, incorporating a hydrogen inhibition term, were obtained for both catalysts. The following kinetic equations were developed: (i) catalyst HT-400 E, $R_1 = 2.799 \times 10^{10} \exp(-34970/RT)P_{H_2}C_S^{1.9}/(1 + 0.0036P_{H_2})$; (ii) catalyst ICI-41-6, $R_2 = 4.962 \times 10^{10} \exp(-32590/RT)P_{H_2}C_S^{2.3}/(1 + 0.0050P_{H_2})$. Evaluations of effectiveness factors and effective diffusion coefficients reported in this paper and associated with the use of particular catalyst pellet sizes were based on HDS standard experiments.

The recent developments in residuum hydroprocessing reflect the worldwide trends in product demands and crude oil quality. The challenge of the 1980s for the petroleum industry is to convert more of the heaviest portion of crude oil into more valuable fuels. Residuum hydroprocessing will contribute in a decisive way to the new refinery requirements and the widespread needs for oil products of an improved quality.

One of the most important methods of hydrotreating an oil residue is the direct catalytic hydrodesulfurization because of its effectiveness in reducing sulfur, nitrogen, metals, and oxygen contents and also in improving the quality of the hydrodesulfurized feedstocks. A considerable number of studies on residue HDS have appeared in the literature. Gates et al. (1979), Crynes (1977), and Schuman and Shalit (1970) reviewed the general aspects of the hydrodesulfurization process. Hirotsugu et al. (1980) and Cecil et al. (1968) discussed the HDS of different Middle East atmospheric residues in terms of the plug flow assumption, with a second-order kinetics with respect to sulfur concentration in both a microreactor and a pilot trickle bed reactor. Beuther and Schmidt (1963) reported a mechanism and kinetics of HDS of high sulfur Middle East reduced crude. They proposed that the simple second-order reaction rate model was adequate for expressing the kinetics of HDS processing. Papayannakos and Marangozis (1984) studied HDS of Thasos atmospheric residue by using a fix bed recycle reactor and deduced a $n = 2.5$ kinetic order. The nature of the sulfur compounds present in petroleum residuum is discussed by Schuit and Gates (1973), Corbet (1969), Dickie and Teh (1967), Drushell (1972), and Richardson and Alley (1975). Hirotsugu et al. (1982) used the gel permeation chromatography (GPC) technique to investigate the molecular size distribution of both sulfur and organometallic metal compounds in various Middle East atmospheric residues. They concluded that the major portion of these atmosphere residues consisted of compounds of a molecular weight below 700

0888-5885/87/2626-0494$01.50/0

and also that molecules of a size less than the *GPC extended chain length of 50* Å occupied about 80–90% of the residues under consideration. Hirotsugu et al. (1979) discussed the relation between the HDS and the various side reactions (asphaltenes and metal removal of different types of residue feedstocks and concluded that the apparent activation energies (E) were 25–30, 16, 20, and 26 kcal/mol for sulfur, asphaltene, vanadium, and nickel removal, respectively.

The primary aim of this work is the investigation of the catalytic kinetics of the HDS of Thasos atmospheric residue under complete mixing conditions, ensuring the liquid-phase homogeneity as regards temperature, pressure, and sulfur concentration. The analysis of trickle bed reactor kinetic data based on a plug flow assumption might be influenced by incomplete wetting due to channelling, axial backmixing, and the competing effects of the interparticle mass transfer. The use of a spinning basket reactor provides the experimental means to minimize the aforementioned drawbacks associated with the operation of a trickle bed contacting system. To our knowledge, a spinning basket reactor type has not been used for HDS studies with oil atmosphere residue, although in at least one case (Myers and Robinson, 1978) was used in a relevant study of a model sulfur compound (dibenzothiophene in white oil).

Kinetic studies reported in this article were carried out on two commercial HDS catalysts: (a) HT-400 E (Harshaw Chemical Co.) and (b) ICI-41-6 (Imperial Chemical Industries, P.L.C., England). HT-400 E catalyst was recently used by Papayannakos and Marangozis (1984) in HDS kinetic studies of Thasos atmospheric residue on a trickle bed recycle reactor. Comparisons of kinetic equations deduced from both reactor systems using the same catalyst type, particle size, and practically comparable experimental conditions are presented in the Results and Discussion section of this work. The use of the ICI-41-6 catalyst was decided in order to investigate the effect of the differences in chemical and physical properties of two catalysts upon the HDS kinetic parameters.

The HDS kinetic data reported here is a part of the results of a broader research program dealing with the investigation of catalyst deactivation phenomena associated with the use of the aforementioned raw materials and catalysts (Ammus, 1985).

Theory

Previously Proposed HDS Kinetic Models. Recent work reported (Gates et al., 1979) in the field of HDS kinetics established that the kinetics of the thiophene (T) hydrodesulfurization reaction can be satisfactorily described by the Hougen–Watson kinetic equation, an extension of the earlier Langmuir–Hinshelwood kinetic model

$$R_{HDS} = kp_T p_{H_2}/(1 + K_T p_T + K_{H_2S} p_{H_2S})^2 \quad (1)$$

for thiophene disappearance (hydrogenolysis) and

$$R_{hyd} = k' p_B p_{H_2}/(1 + K_B' p_B + K_{H_2S} p_{H_2S}) \quad (2)$$

for butane formation (butene hydrogenation).

Further studies involving more complex model sulfur compounds, i.e., benzothiophene (BT), dibenzothiophene (DBT), etc., were accomplished. Myers and Robinson (1978) used a spinning basket reactor type to investigate the kinetics of the hydrodesulfurization of sulfur model compounds (DBT). It was found that the kinetic model which described the behavior of the HDS reaction had the form

$$R_{DBT} = kp_{DBT} p_{H_2}{}^n/(1 + K_{DBT} p_{DBT} + K_{H_2S} p_{H_2S}{}^m) \quad (3)$$

By nonlinear regression techniques, the best fitting of the data was obtained for $n = 1$ and $m = 1$ or 2. It was also found that the reaction rate was not strictly first order with respect to DBT. Reaction network studies of the HDS of DBT, carried out by Houalla et al. (1978) in a high-pressure flow microreactor, showed that the conversion data were generally consistent with that for a pseudo-first-order reaction for each of the organic reactants. Broderick and Gates (1981) analyzed the reaction kinetics of both the hydrodesulfurization and the hydrogenation reactions of DBT, using an isothermal plug-flow reactor. The kinetics of the two primary reactions of DBT can be summarized in the followed recommended rate equations determined from differential conversion data.

$$R_{HDS} = k' K_{DBT} K_{H_2} C_{DBT} C_{H_2}/(1 + K_{DBT} C_{DBT} + K_{H_2S} C_{H_2S})(1 + K_{H_2} C_{H_2}) \quad (4)$$

$$R_{hyd} = k' K_{DBT} K_{H_2} C_{DBT} C_{H_2}/(1 + K_{DBT} C_{DBT}) \quad (5)$$

Research work carried out at Amoco by Frye and Mosby (1967) dealt with HDS reaction rate studies on single sulfur compounds in light catalytic cycle oil by means of a trickle bed reactor and first-order reaction kinetics with respect to hydrogen and the reactant model sulfur compound. The following kinetic model was used:

$$R_{HDS} = kp_s p_{H_2}/(1 + K_{Ar} p_{Ar} + K_{H_2S} p_{H_2S})^2 \quad (6)$$

Papayannakos and Marangozis (1984) studied the kinetic of the hydrodesulfurization of atmospheric residue of Thasos oil by means of a trickle bed batch recycle reactor. The recommended rate equation established from an analysis of the HDS conversion data was

$$R_{HDS} = kp_{H_2} C_S{}^n/(1 + K_{H_2} p_{H_2} + K_{H_2S} p_{H_2S}) \quad n = 2.5 \quad (7)$$

Theoretical Treatment

The proposed theoretical kinetic model in this work is essentially based on a simplified form of the Hougen–Watson kinetic equation

$$R_{HDS} = k_v p_{H_2} C_S{}^n/(1 + K_{H_2} p_{H_2}) \quad (8)$$

assuming $p_{H_2S} \simeq 0$.

The determination of the constants n, k_v, and K_{H_2} is based on differential conversion data from model experiments done on a spinning basket reactor type (Ammus, 1985). The analysis of the experimental results included the following mass balance valid for the reactor volume

$$R_{HDS} W_{cat} = -V_{oil} \frac{dC_S}{dt} \quad (9)$$

which is transformed into

$$\frac{dS_k}{S_k{}^n} = k\left(\frac{W_{cat} \rho_{oil}{}^n}{W_{oil}(3200)^{n-1}}\right) dt \quad (10)$$

where

$$k = k_v P_{H_2}/(1 + K_{H_2} P_{H_2}) \quad (11)$$

and

$$S_k = \left(\frac{3200}{\rho_{oil}}\right) C_S \quad (12)$$

On integration of (10) we get

$$\frac{1}{S_{k(t)}^{n-1}} - \frac{1}{S_{k(0)}^{n-1}} = k\left(\frac{(n-1)\rho_{oil}{}^n W_{cat}}{3200^{n-1} W_{oil}}\right) t \quad (13)$$

Table I. Atmospheric Residuum Feedstock Characteristic Properties (Crude of Prinos, Thasos)

property	Thasos atm residue
specific gravity, 15/4 °C, g/cm³	1.007
°API	9
content, wt %	5.6
kinematic viscosity, 122 °F, cSt	235
C residue (Conradson), wt %	14.3
V, ppm	9[a]
Ni, ppm	11[a]
boiling range, °C	+315
yield of crude, wt %	51

[a] Papayannakos and Marangozis, 1984.

$S_{k(t)}$ is the corrected experimental sulfur content (S_{exptl} wt %) due to sampling and minor liquid lost in the form of droplets carried away by the effluent gases.

The relation between $S_{k(t)}$ and S_{exptl} is

$$S_{k(t)_{i=1,2...,\nu}} = S_{k_{i-1}} - \left(\frac{W_{i-1}}{W_0}\right)(S_{exptl(i-1)} - S_{exptl(i)})\left(\frac{S_{k_{i-1}}}{S_{exptl(i-1)}}\right)^n \quad (14)$$

where W_{i-1} is the mass of oil in the reactor after the ith sampling (g), W_0 is the original mass of oil in the reactor (g), and ν is the total number of samples.

Model equation (13) can be used in the linear regression procedure involving the plotting of $[(1/S^{n-1}_{k(t)}) - (1/S^{n-1}_{k(0)})]$ vs. t to determine specific reaction rate constant k for an assumed kinetic order n. Standard errors of correlation associated with assumed values of reaction order (n) are calculated. The best value of n corresponding to the minimum standard error of correlation is considered as the HDS reaction order.

Experimental Section

Materials Used. Samples of crude oil from Prinos wells (Thasos) were distilled under atmospheric conditions in a laboratory distillation apparatus (Hempel type) to obtain the residue feedstock. The basic characteristic properties of this raw material are cited in Table I.

The catalyst used were (a) the commercial grade HT-400 E-H08 and -H109, supplied by Harshaw Chemie, Bv, De Meern, Holland, in the form of cylindrical extrudates Φ 1.62 × 3.4 mm and Φ 3.3 × 4.77 mm and particles of an average diameter 0.34 mm (30–40-mesh US sieves) obtained by crushing the pellets and (b) the ICI-41-6 commercial grade supplied by Imperial Chemical Industries, P.L.C., England, in the form of cylindrical extrudates Φ 1.46 × 3.02 mm and crushed pellets of an average diameter 0.34 mm.

Pore structure parameters of the catalysts used in this study are reported in Tables II and III. Hydrogen (a commercial grade $H_2 + D_2$ >99.8% purity) was supplied by Air Liquide Hellas.

Spinning Basket Reactor. An illustration of the spinning basket reactor showing mechanical design details is presented in Figure 1. The spinning basket consists of four orthogonal beds with their longer dimension being vertically oriented and fixed at a symmetric position on a horizontally rotating disk. The dimensions of each bed are 30, 25, and 11 mm, and the total volume of the spinning catalyst basket is V_{cb} = 33 cm³. The catalyst is held in place by an inoxidable wire mesh, inside the basket bed skeleton. Catalyst beds are surrounded by a system of eight baffles at symmetric positions, directing the fluid flow and preventing liquid vortexing. A cylindrical autoclave of an interior volume of V_R = 888 cm³, designed and built at the Laboratory of Chemical Process Engineering (NTU), works as the heart of the reactor system and is equipped with an electromagnetic drive to rotate the basket. The inside diameter of the autoclave is 120 mm, and its height is 80 mm.

A set of three electric resistances connected in parallel is used to heat up the autoclave peripherally, while the bottom side of the autoclave is heated by another electric resistance.

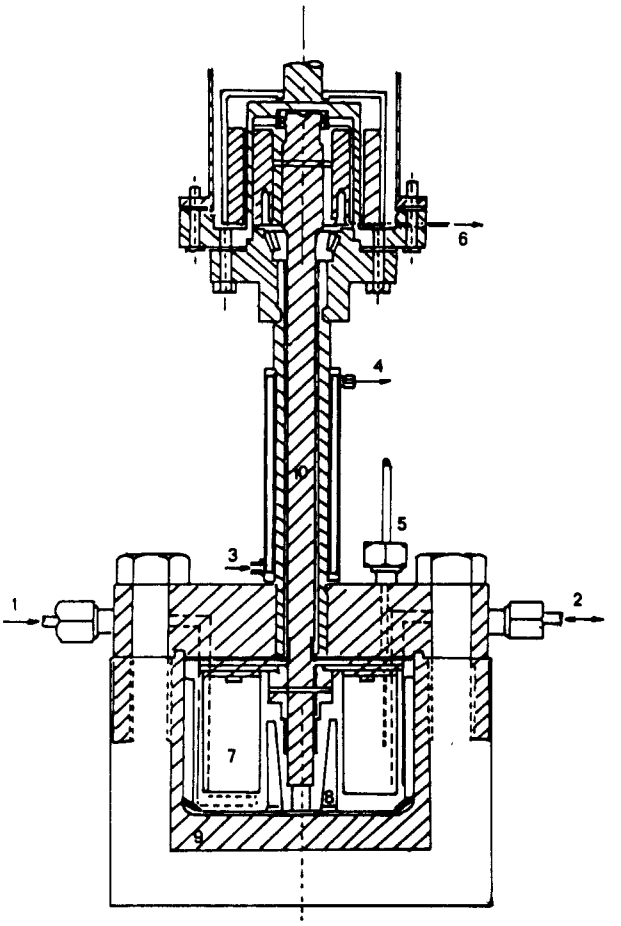

Figure 1. Mechanical design details of the spinning basket reactor: (1) hydrogen inlet, (2) oil residue charge–discharge and sampling point, (3) water inlet, (4) water outlet, (5) thermocouple sheath, (6) gas product exit, (7) catalyst basket, (8) baffle, (9) autoclave body (pressure vessel), and (10) rotating shaft.

Experimental System Description. Auxiliary equipment to support reactor operation are shown in

Table II. Pore Structure Parameters of the HDS Catalysts Used in This Work

	specific pore surface area, m²/g			specific pore vol, cm³/g			most probable pore diameter, Å	
catalyst type (before use)	Hg[a]	N_2[b]	CS[c]	Hg	N_2	CS	Hg	N_2
HT-400 E-H08 ($^1/_{16}$ in.)	133	215	230	0.36	0.44	0.50	106	86
HT-400 E-H109 ($^1/_8$ in.)	123	218	230	0.34	0.44	0.50	108	82
ICI-41-6 ($^1/_6$ in.)	190	253	250	0.50	0.50	0.55	99	74

[a] Determined by mercury penetration. [b] Determined by nitrogen adsorption. [c] Value provided by catalyst supplier (CS).

Table III. Specifications Concerning Catalyst Chemical Composition (Provided by the Supplier). Physical Characteristics

property	type of commercial catalyst		
	HT-400 E		
	H08	H109	ICI-41-6
CoO, wt %	3.0	3.0	3.3
MoO_3, wt %	15	15	14
Al_2O_3, wt %	balance	balance	balance
bulk density, g/cm^3	1.30	1.25	1.27
particle size, in.	$^1/_{16}$	$^1/_8$	$^1/_{16}$
mean mechanical strength	6	6	5.5
bed bulk density, g/cm^3	0.77	0.74	0.77
void fraction of catalyst bed	0.412	0.409	0.472

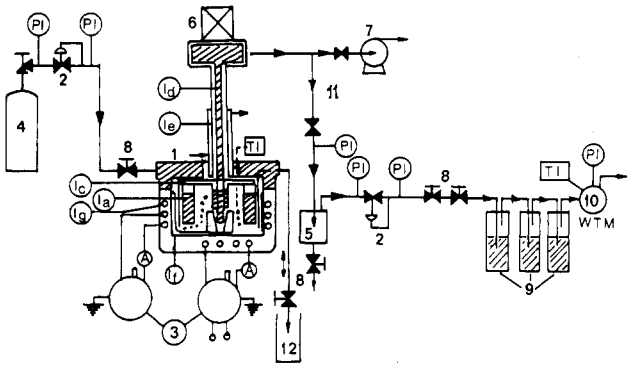

Figure 2. Flow diagram of the experimental apparatus. The reactor is shown in the center, surrounded by temperature, pressure, and flow control valves: PI, pressure indicator; TI, temperature indicator; Ia, catalyst basket; Ib, baffles; Ic, rotating disk; Id, rotating shaft; Ie, heat exchanger; If, autoclave; Ig, electric resistance; (1) reactor; (2) pressure control valves; (3) variable transformer (Variac); (4) hydrogen pressure cylinder; (5) high-pressure phase separator; (6) drive motor; (7) vacuum pump; (8) needle valve; (9) gas scrubbers; (10) wet test meter; (11) on–off manual valves; (12) feed tank.

Figure 2. A constant hydrogen flow through the reactor is achieved by a pair of flow control valves (Figure 2, 8) and a pressure reducer (Figure 2, 2) installed at the exit stream. Hydrogen sulfide is removed from the effluent gas by passing the gas stream through a sequence of three glass scrubbers containing, successively, (a) white oil to remove vaporized oil, (b) a NaOH solution to neutralize H_2S, and (c) a $CdSO_4$ solution to detect the saturation of the NaOH solution contained in the preceding scrubber. If traces of H_2S are allowed to reach the $CdSO_4$ scrubber, the formation of an intense yellow precipitate of CdS is immediate. The effluent gas is subsequently flowing through a wet test meter that measures the gas flow rate.

Model HDS Experiments. Model HDS experiments were carried out to investigate the effect of process variables (temperature, hydrogen partial pressure, and rate of agitation) upon the rate of the hydrodesulfurization reaction. Both catalysts were employed in their pulverized form, having an average equivalent particle size of 0.34 mm. Basic process variables assumed the following standard values: temperature, T = 350 °C; hydrogen partial pressure, p_{H_2} = 50 bar; hydrogen volumetric flow rate at the exit stream, Π_{H_2} = 60 L/h; rate of agitation, ω = 2900 rpm; and liquid feedstock, Thasos atmospheric residue (+315 °C).

The temperature was raised and maintained at 350 °C, and the pressure was controlled at 50 bar. Hydrogen volumetric flow rate in the gas exit was about Π_{H_2} = 60 L/h, sufficient to keep the H_2S concentration in the gas effluent well below a level ensuring the minimization of H_2S inhibition effects. Sampling of desulfurized liquid could be done directly from the reaction space, and sulfur concentration was being determined by an X-ray fluorescence facility (Telsec Laboratory X-100, Analex Company Ltd., U.K.). Kinetic experiments include variations of process variables one at a time while the remaining basic variables were kept at their standard values. Individual process variables operated over a range as follows: temperature, 280–395 °C; hydrogen partial pressure, 30–70 bar; and agitation, 0–2900 rpm.

Catalyst samples were dried at 400 °C (atmospheric conditions) for 24 h and then charged to the basket beds. The reactor interior was evacuated (~20 torr) at 300 °C for a period of t = 30 min. Catalyst reduction was accomplished by passing a hydrogen stream of 6 L/h, for 3 h, at 250 °C and 8-bar pressure while presulfidation took place in situ at normal experimental conditions which included the charge of the appropriate amount of oil, a hydrogen flow rate of 60 L/h, a temperature T = 350 °C, and a rate of catalyst rotation ω = 2900 rpm. The duration of this run was 10 h.

About 500 g of oil residue was preheated before it was pumped into the reactor. Reaction conditions were then fixed and continuously controlled at the desired values. Desulfurized oil samples of 7–12 g (4 g was required for sulfur determination) were taken at intervals depending on the severity of experimental conditions, i.e., at T = 395 °C or p_{H_2} = 70 bar; the time interval between successive samples was between 25 and 45 min, while at standard conditions (T = 350 °C and p_{H_2} = 50 bar) the sampling time was between 60 and 100 min. Individual experimental runs had a duration between 480 and 600 min. Used catalyst samples and desulfurized oil were discharged and renewed upon the completion of a particular run.

The effects of catalyst particle size upon HDS reaction rate were investigated under standard experimental conditions, using catalyst particles with a varying characteristic length, $\bar{L}_p$, defined by $\bar{L}_p = V_p/S_x$; i.e., for HT-400 E, $\bar{L}_p$ = 0.00584–0.05670 cm, and for ICI-41-6, $\bar{L}_p$ = 0.00589–0.02940 cm. Effectiveness factors and average effective diffusion coefficients were determined.

Results and Discussion

The objectives of this study were 1. to evaluate the reactor performance and determine the minimum agitation rate to render the process controlled by chemical reaction and 2. to confirm earlier hydrodesulfurization kinetics developed by other researchers on both selected model sulfur compounds in light hydrocarbon solvents (Frye and Mosby, 1967; Myers and Robinson, 1978) and atmospheric residues by using a trickle bed (Scamangas et al., 1982; Papayannakos and Marangozis, 1984). (Original experimental data are provided as supplementary material.)

Agitation Tests (Catalyst Basket Rotation). The observed HDS reaction rate should represent the catalytic kinetics, free of transport phenomena of reactants (hydrogen and sulfur compounds) through the stagnant film surrounding the catalyst particles. Minimum agitation rates can be established from a set of diagnostic tests in which the HDS rate is measured for different levels of stirring. The rate of agitation was varied between ω = 0 and 2900 rpm, and the HDS rate was measured. Results from these tests are shown in Figure 3 (numerical results are given as supplementary material). The raising of the agitation rate from ω = 0 to 2450 rpm caused an increase of the HDS rate by about 54%. A further rise of the agitation rate from ω = 2450 to 2540 rpm resulted in a minor increase of the HDS reaction rate (5%), while a final rise to ω = 2900 rpm caused a negligible (~1%) increase of the HDS rate, in the sense that it was within experimental error. It is concluded that ω = 2540 rpm should

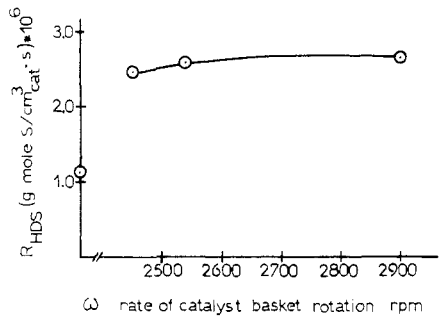

Figure 3. Effect of catalyst rotation rate upon the HDS reaction rate.

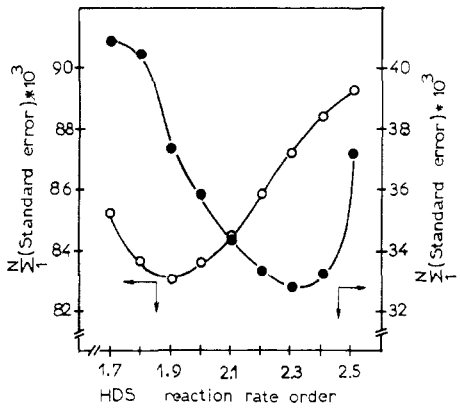

Figure 4. Schematic presentation of the sum of standard errors of fitting the HDS kinetic model over the pertinent experimental data: T = 350 °C, P_{H_2} = 50 bar, Π_{H_2} = 60 L/h, ω = 2900 rpm, and d_p = 0.34 mm, (⊙) catalyst HT-400 E, and (●) catalyst ICI-41-6.

be an adequate rate of rotation. Experiments were carried out at ω = 2900 rpm to ensure a satisfactory mixing also.

Reaction Order. Equation 13 was used in a linear regression analysis of the experimental data (total sulfur concentration decreasing with operating time) obtained under standard conditions (T = 350 °C, p_{H_2} = 50 bar, ω = 2900 rpm, Π_{H_2} = 60 L/h); optimum reaction order values were determined graphically from the plots appearing in Figure 4 (relevant experimental results are found in supplementary material). Reaction orders n_1 = 1.9 and n_2 = 2.3 were evaluated for catalysts HT-400 E and ICI-41-6, respectively.

The HDS reaction order with respect to sulfur concentration has been reported to be a function of the physicochemical properties of the reactant material, the composition and chemistry of the individual sulfur compounds (Beuther and Schmidt, 1963; Scamangas et al., 1982; Cecil et al., 1968), and the effectiveness of liquid–solid catalyst contacting (Weekman, 1976) as well as the degree of desulfurization (Bridge et al., 1979; Scott and Bridge, 1970). The HDS reaction order reported in the literature showed a variety of values ranging from 1.0 to 2.5. For Thasos atmospheric residue HDS, Papayannakos and Marangozis (1984) suggested that the integral reactor experimental results are not sufficient to discriminate order values in the range 2.0–2.5. They also concluded that a batch recycle reactor is a suitable system to effect such a discrimination and calculated a reaction order n = 2.5 by best fitting a kinetic model to experimental data obtained on HT-400 E catalyst at standard experimental conditions (T = 350 °C, p_{H_2} = 50 bar, in a batch recycle reactor system). The proposed value is considered to be high and may be a reflection of a number of process features like the type of catalyst bed (being fixed and not moving or rotating), the effectiveness of solid–liquid contacting, the degree of desulfurization, and finally the precision in the evaluation

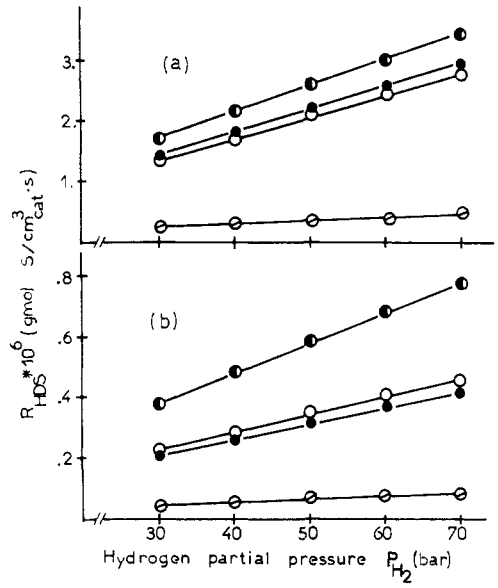

Figure 5. Comparison of HDS rates at various operating pressures, valid for Greek oil residue. Catalyst particle size d_p = 0.34 mm. Catalyst grades used: (⊖) COMOX 451, T = 350 °C, trickle bed continuous reactor (Scamangas et al., 1982); (●) HT-400 E, T = 350 °C, batch recycle reactor (Papayannakos and Marangozis, 1984); (◐) HT-400 E and (⊙) ICI-41-6, T = 350 °C, ω = 2900 rpm (this work). Total sulfur concentration: (a) S = 5.5% w/w (C_S = 1.42 × 10^{-3} g-mol of S/cm³ of oil) and (b) S = 2.5% w/w (C_S = 0.64 × 10^{-3} g-mol of S/cm³ of oil).

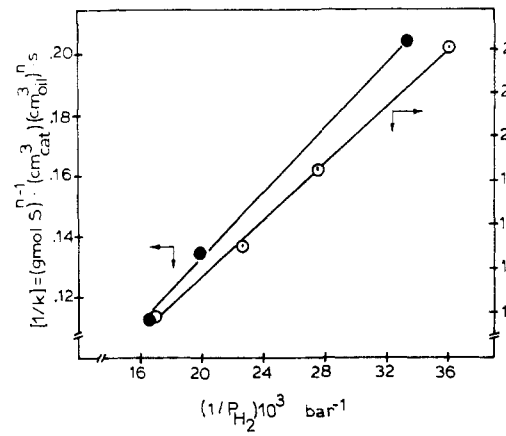

Figure 6. Effect of hydrogen partial pressure upon the specific reaction rate k: T = 350 °C, Π_{H_2} = 60 L/h, ω = 2900 rpm, and d_p = 0.34 mm, (⊙) catalyst HT-400 E, and (●) catalyst ICI-41-6. Slope and intercept can be used in the evaluation of K_1 and k_v according to formula $1/k = K_1/k_v + (1/k_v)(1/P_{H_2})$.

of the effective sulfur concentration. The spinning catalyst basket reactor offers obvious advantages and improves markedly the aforementioned sources of uncertainty. Sampling is carried out directly from the reaction space surrounding the active catalyst, while sulfur concentration errors due to sampling are systematically corrected.

In conclusion, model HDS kinetic experiments carried out on a spinning basket reactor, using the same catalyst and pratically identical experimental conditions, led to a reaction order lower by approximately 0.6 of a unit in comparison with values obtained in a fix bed catalytic reactor. Catalyst type, other factors being constant, imparts its influence on the reaction rate order.

Effect of Hydrogen Partial Pressure. A linear change of HDS reaction rate with hydrogen partial pressure was observed for both catalysts with only a slight deviation in the region of high pressures (over 55–60 bar), Figure 5 (◐ and ○ lines). Hydrogen inhibition effects can

Table IV. Activation Energies of the HDS of Thasos Atmospheric Oil Residue Feedstock

type of commercial grade catalyst	type of reactor and mode of operation	activation energy, kcal/mol	ref
CoMoX 451	fixed bed (integral trickle bed flow reactor)	29.0	Scamangas et al., 1982
HT-400 E	batch recycle trickle bed reactor	36.1	Papayannakos and Marangozis, 1984
HT-400 E	batch spinning basket reactor	35 ± 1	this work
ICI-41-6	batch spinning basket reactor	32 ± 1	this work

be best correlated (Figure 6) by the $k = k_v p_{H_2}/(1 + K_{H_2} p_{H_2})$, where k is the intrinsic rate constant and K_{H_2} is the hydrogen adsorption equilibrium coefficient.

The mean hydrogen sulfide molar ratio varied over the range $y_{H_2S} = 0.01–0.08$, while the relevant mean partial pressure in the gas product varied over the range $P_{H_2S} = 0.4–2$ bar, which is equivalent to between 0.8% and 2.8% of the total applied pressure. The precentage of sulfur removed per hour was below 10% of the total amount of sulfur present in the liquid phase.

A linear regression analysis yielded the values $K_1 = 0.0036$ bar^{-1} and $K_2 = 0.0050$ bar^{-1} for the HT-400 E and ICI-41-6 catalysts, respectively, indicating that apart from the reactive sites, active sites are occupied by adsorbed hydrogen according to the Langmuir type adsorption model. Hydrogen inhibition effects are more intensive in ICI-41-6 catalyst than in HT-400 E (for numerical results, refer to supplementary material).

Effect of Temperature. In light of the information presented in the previous section, the global rate equation, given in eq 8, assumes the forms

$$R_I = k_{v_1} p_{H_2} C_S^{1.9}/(1 + 0.0036 p_{H_2}) \quad (15)$$

for HT-400 E catalyst and

$$R_{II} = k_{v_2} p_{H_2} C_S^{2.3}/(1 + 0.00496 p_{H_2}) \quad (16)$$

for ICI-41-6 catalyst.

For reliable determinations of temperature effects upon the intrinsic reaction rate, one should be careful to ensure the absence of external mass-transfer limitations, an effectiveness factor $\eta = 1$, and experimental results to be free of any deactivation phenomena (catalyst intrinsic activity $\epsilon = 1$); that is, $\eta\epsilon = 1$. It is also important to control a constant hydrogen pressure, a negligible hydrogen sulfide partial pressure. The experiments were done on crushed catalyst pellets of both catalysts with an average particle characteristic length $\bar{L}_p = 0.00586$ cm at temperatures varying between $T = 285$ and 395 °C for the ICI-41-6 catalyst, at $p = 50$ bar. Arrhenius plots are shown in Figure 7, where the apparent reaction rate constant $k = k_v p_{H_2}/(1 + K_L p_{H_2})$ (being directly proportional to k_v) vs. the reciprocal absolute temperature are drawn. The following analytical Arrhenius expressions were derived

$$k_1 = 1.1860 \times 10^{12} \exp(-17574/T) \quad (17)$$

$$k_2 = 1.988 \times 10^{12} \exp(-16396/T) \quad (18)$$

Equation 17, valid for HT-400 E catalyst, is in fairly good agreement with the pertinent correlation; i.e., $k = 3.63 \times 10^{12} \exp(-18168/T)$, deduced from the Arrhenius plot reported by Papayannakos and Marangozis (1984), who tested the same oil and catalyst type on a batch-recycle trickle bed reactor.

The calculated overall activation energies were 35 ± 1 and 32 ± 1 kcal/mol for HT-400 E and ICI-41-6 catalysts, respectively. These values indicate that surface hydrogenolysis reactions may be the rate-determining step. It can also be seen from the Arrhenius diagram valid for ICI-41-6 catalyst (Figure 7) that at higher temperatures a transition to intraparticle diffusion control is favored,

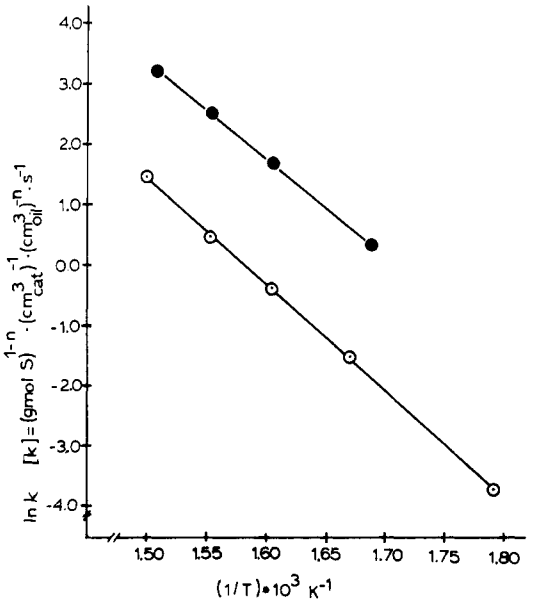

Figure 7. Effect of temperature upon the specific reaction rate of the HDS of Thasos oil residue: $P_{H_2} = 50$ bar, $\Pi_{H_2} = 60$ L/h, $\omega = 2900$ rpm, and $d_p = 0.34$ mm, (⊙) catalyst HT-400 E, and (●) catalyst ICI-41-6.

indicating a higher increase of the chemical reaction rate, due to temperature rise, in comparison with that of physical transport phenomena.

Activation energies concerning the HDS of Thasos oil residue reported in the literature are given in Table IV and are compared with values reported in this work. Finally intrinsic reaction rate constants k_v can be computed via eq 19 and 20 which were deduced by substitution of eq 17 and 18 for k (i.e., $k = k_v P_{H_2}/(1 + K_{H_2} P_{H_2})$)

$$k_{v1} = 2.799 \times 10^{10} \exp(-17.574/T) \quad (19)$$

k_{v1} = (cm^3 of oil)$^{1.9}$ mol$^{-0.9}$ (cm^3 of catalyst)$^{-1}$ s^{-1} bar^{-1}

$$k_{v2} = 4.962 \times 10^{10} \exp(-16.396/T) \quad (20)$$

k_{v2} = (cm^3 of oil)$^{2.3}$ mol$^{-1.3}$ (cm^3 of catalyst)$^{-1}$ s^{-1} bar^{-1}

Comparisons of Greek oil residue HDS reaction rates vs. the operating pressure on various catalyst grades are depicted in Figure 5.

Effect of Particle Size. The following particle sizes of both catalysts studied in this work were used to investigate the intraparticle diffusion phenomena: catalyst HT-400 E, $\bar{L}_{p_0} = 0.00567$ cm (pulverized, $d_p \simeq 0.34$ mm), $\bar{L}_{p_1} = 0.0326$ cm ($d_p = {}^1/_{16}$ in.), and $\bar{L}_{p_2} = 0.0589$ cm ($d_p = {}^1/_8$ in.); catalyst ICI-41-6, $\bar{L}_{p_0} = 0.00567$ cm (pulverized, $d_p \simeq 0.34$ mm) and $\bar{L}_{p_1} = 0.0294$ cm ($d_p = {}^1/_{16}$ in.).

The determination of both the effectiveness factor and the effective diffusivity is based on the global reaction rates measured on newly activated catalyst, samples ($\epsilon = 1$) of the aforementioned particle sizes.

The observed specific HDS reaction rate constant k_{obsd} is defined by $k_{obsd} = k_v \epsilon \eta$. The values of k_v for the two catalysts are given in eq 19 and 20, catalyst activity assumed to be $\epsilon = 1$, since global HDS rates were measured

soon after catalyst activation. The estimation of the effectiveness factor η which is a function of the generalized Thiele modulus Φ defined by

$$\Phi = \bar{L}_p((n + 1)k\epsilon C_S^{n-1})/(2D_{eff})^{1/2} \quad (21)$$

(Froment and Bischoff, 1979) where Φ = generalized Thiele modulus, $\bar{L}_p$ = characteristic length defined as the ratio of the particle volume upon the external particle surface area, ϵ = relative catalyst activity ($\epsilon = 1$), n = reaction order, k = specific reaction rate, $k = k_v p_{H_2}/(1 + K_i p_{H_2})$, and D_{eff} = sulfur compound effective diffusivity (cm^2/s), is achieved by using a trial-and-error calculating technique.

For catalyst HT-400 E, the observed HDS global rates R_0, R_1, and R_2, valid for characteristic lengths $\bar{L}_{p_0}$, $\bar{L}_{p_1}$, and $\bar{L}_{p_2}$, and the known function $\eta = f(\Phi)$ are involved in effectiveness factor determinations.

Thus, the following equations can be formulated

$$\frac{R_0}{R_1} = \frac{\eta_0}{\eta_1} \qquad \frac{R_0}{R_2} = \frac{\eta_0}{\eta_2} \quad (22)$$

$$\frac{\bar{L}_{p_0}}{\bar{L}_{p_1}} = \frac{\Phi_0}{\Phi_1} \qquad \frac{\bar{L}_{p_0}}{\bar{L}_{p_2}} = \frac{\Phi_0}{\Phi_2} \quad (23)$$

An initial guess $\eta_0 = 1$ is made, η_1 and η_2 are determined through eq 22, and Φ_0, Φ_1, and Φ_2 are determined from the relevant $\eta = f(\Phi)$ correlation. The trial is repeated with a new value $\eta_1 = \eta_0 - 0.01$ until eq 22 and 23 are satisfied.

The following values were yielded for the two catalysts: catalyst HT-400 E, $\eta_0 = 0.97$ ($\Phi_0 = 0.42$), $\eta_1 = 0.46$ ($\Phi_1 = 2.0$), $\eta_2 = 0.21$ ($\Phi_2 = 4.7$); catalyst ICI-41-6, $\eta_0 = 0.90$ ($\Phi_0 = 0.65$), $\eta_1 = 0.26$ ($\Phi_1 = 3.4$). Effective diffusivities D_{eff} are calculated through eq 21 solved with respect to D_{eff}. Thus,

$$D_{eff} = (\bar{L}_p/\Phi)^2((n + 1)kC_S^{n-1}/2) \quad (24)$$

The following D_{eff} values were computed:

	$\bar{L}_p$, cm	D_{eff}, cm^2/s
catalyst HT-400 E	0.005 67	3.23×10^{-7}
	0.032 00	4.06×10^{-7}
	0.057 80	2.57×10^{-7}
catalyst ICI-41-6	0.005 67	1.047×10^{-7}
	0.029 40	1.018×10^{-7}

The slightly higher D_{eff} values calculated for catalyst HT-400 E compared with those for catalyst ICI-41-6 might be due to the observed differences in the mean pore size between the two catalyst types. The D_{eff} values reported here are only approximate, and their validity depends on the accuacy of $\bar{L}_p$ and Φ values calculated through eq 21–23.

Direct effective diffusion coefficients measurements on various catalyst particle sizes in the conventional Wick and Kallenback apparatus would yield D_{eff} values to check the validity of the indirectly calculated relevant values.

Catalyst Deactivation. Catalyst deactivation phenomena were observed on all catalyst types and particle sizes used in this investigation and received a thorough quantitative treatment. Relative catalyst activity loss vs. run time curves were derived, rates of coke and metal deposition, pore structure, and overall pore surface and area changes of the used catalyst were correlated with the run time and the relative catalyst activity. An extensive presentation of these results will be the theme of a forthcoming publication. It suffices here to make a general comment on the mode of deactivation which appeared to indicate a roughly linear drop of activity with time. Thus, in a catalyst operating period of 180 h, the activity of catalyst HT-400 E reached the value of 0.4 of its original value, while the corresponding value for ICI-41-6 approached the value of 0.5 of its initial value.

It also deserves mentioning that the HT-400 E catalyst showed an initial activity value 25% higher than the corresponding value for the ICI-41-6 catalyst.

Conclusions

The spinning basket reactor proved to be a fairly successful research tool for the investigation of engineering kinetics in multiphase catalytic systems, under the severe operating conditions applied during hydrotreating of oil residua. It is also considered as demonstrating a superior performance compared with that of a fixed bed reactor in kinetic studies carried out on multiphase catalytic reaction systems and ensuring reliable determinations of HDS intrinsic kinetic parameter, as it is evident from the kinetic studies on Greek atmospheric oil residue. Thus, for sound intrinsic kinetic evaluations, preference should be given to the spinning basket reactor system, despite any operational difficulties, which have to be handled with care.

The usefulness of the fixed bed reactor should not be underrated because research results obtained on such a system reflect the influence of partial wetting and mass- and heat-transfer limitations, implicitly present in industrial fixed bed oil HDS units.

Catalyst particle size and reaction kinetic parameters interactions are mainly dictated by the physical and chemical catalyst properties, prevailing during the usage of the selected catalyst. The differences in physical pore structure of the catalysts used in this work gave rise to variations in the effectiveness factor mode of change under comparable operating and particle size reduction conditions.

Acknowledgment

We thank Harshaw Chemical Co. and Imperial Chemical Industries for the donation of catalyst samples. We also thank the Petroleum Corporation of Greece for supplying the crude oil sample. J.A. acknowledges with thanks the State Scholarships Foundation of Greece for their financial support.

Nomenclature

C_S = sulfur concentration, g-mol of S/cm^3 of oil
D_{eff} = effective diffusion coefficient, cm^2/s
E_i = activation energy ($i = 1$ catalyst HT-400 E, $i = 2$ catalyst ICI-41-6), kcal/mol
k = specific reaction rate constant defined by $k = k_v P_{H_2}/(1 + K_1 P_{H_2})$, (g-mol of S)$^{1-n}$ (cm^3 of catalyst)$^{-1}$ (cm^3 of oil)$^{-n}$ s^{-1}
k_v = intrinsic reaction rate constant, (g-mol of S)$^{1-n}$ (cm^3 of catalyst)$^{-1}$ (cm^3 of oil)$^{-n}$ bar^{-1} s^{-1}
K_A = adsorption equilibrium constant for species A, bar^{-1} (A:B, butene; BT, benzothiophene; DBT, dibenzothiophene; H_2, hydrogen; H_2S, hydrogen sulfide; Ar, aromatics; T, thiophene)
L_p = characteristic catalyst particle length, $\bar{L}_p = V_p/S_x$, cm
n = HDS reaction order with respect to total sulfur concentration
p_A = partial pressure of gaseous species A, bar (A ≡ B, BT, DBT, H_2, H_2S, Ar, and T)
R_{HDS} = rate of hydrodesulfurization, g-mol of S/(cm^3 of catalyst·s)
R_{hyd} = rate of hydrogenation, g-mol/(g of catalyst·s)
S_x = external catalyst particle surface area, cm^2
S_k = corrected sulfur content, g of S/100 g of oil
T = temperature of liquid phase in the reactor, °C
t = reaction time, s
$V_{cat.bed}$ = volume of catalyst bed, cm^3
V_{oil} = volume of oil in the reactor, cm^3
V_p = volume of the catalyst particle, cm^3

V_R = reactor volume, cm^3
W_{cat} = mass of catalyst, g
W_{oil} = mass of oil in the reactor, g
y_{H_2S} = hydrogen sulfide molar ratio

Greek Symbols

ϵ = catalyst relative activity (intrinsic)
η = effectiveness factor
ν = number of samples taken during a single HDS experiment
Π_{H_2} = hydrogen volumetric flow rate, L/h
ρ_{oil} = oil density, g of oil/cm^3 of oil
ω = rate of catalyst basket rotation, rpm

Supplementary Material Available: Original experimental data and numerical results of agitation and HDS rates and optimum reaction order values (11 pages). Ordering information is given on any current masthead page.

Literature Cited

Ammus, J. M. Ph.D. Thesis, National Technical University of Athens, 1985.
Beuther, H.; Schmidt, B. K. Presented at the 6th World Petroleum Congress, Frankfurt/Main, May 19-26, 1963; section III, paper 20-PD7.
Bridge, A. G.; Reed, E. M.; Tamm, P. W.; Cash, D. R. Presented at the 74th National Meeting American Chemical Society, New Orleans, March, 1979; paper 14a.
Broderick, D. H.; Gates, B. C. *AIChE J.* **1981**, *27*(4), 663.
Cecil, R. R.; Mayer, F. X.; Cart, E. N., Jr. Presented at the Annual Meeting of the AIChE, Los Angeles, Dec 1-5, 1968.
Corbet, L. W. *Anal. Chem.* **1969**, *41*, 576.
Crynes, B. L. *Chemical Reactions as a Means of Separation*; Marcel Dekker: New York and Basel, 1977; pp 2-32.
Dickie, J. P.; Teh, Fu Yen *Anal. Chem.* **1967**, *39*(14), 1847.
Drushell, H. V. *Prepr.—Am. Chem. Soc., Div. Petrol. Chem.* **1972**, *17*(4), F 92.P.F (92).
Froment, G. F.; Bischoff, K. B. *Chemical Reactor Analysis and Design*; Wiley: New York, 1979.
Frye, B. C.; Mosby, J. F. *Chem. Eng. Prog.* **1967**, *63*(9), 66.
Gates, B. C.; Katzer, J. R.; Schuit, G. C. A. *Chemistry of Catalytic Processes*; McGraw Hill: New York, 1979; Chapter 5, p 390.
Hirotsugu, Nomura; Yasuo, Sekido; Yutaka, Ohguchi *J. Jpn. Petrol. Inst.* **1979**, *22*(5), 296.
Hirotsugu, Nomura; Yasuo, Sekido; Yutaka, Ohguchi *J. Jpn. Petrol. Inst.* **1980**, *23*(5), 321.
Hirotsugu, Nomura; Tetsuo, Satoh; Yasuo, Sekido *J. Jpn. Petrol. Inst.* **1982**, *25*(1), 1.
Houalla, M.; Nag, N. K.; Sapre, A. V.; Broderick, T.; Gates, B. C. *AIChE J.* **1978**, *24*(6), 1015.
Myers, E. C.; Robinson, K. K. Presented at the 5th International Symposium on Chemical Reaction Engineering, Houston, March 13-15, 1978; *ACS Symp. Ser.* **1978**, *65*, 1.
Papayannakos, N.; Marangozis, J. *Chem. Eng. Sci.* **1984**, *39*(6), 1051.
Richardson, R. L.; Alley, S. K, *Prep.—Am. Chem. Soc., Div. Petrol. Chem.* **1975**, *20*(2), 554.
Scamangas, A.; Papayannakos, N.; Marangozis, J. *Chem. Eng. Sci.* **1982**, *37*(12), 1812.
Schuit, G. C. A.; Gates, B. C. *AIChE J.* **1973**, *19*(3), 417.
Schuman, S. C.; Shalit, H. *Catal. Rev.* **1970**, *4*, 245.
Scott, J. W.; Bridge, A. G.; Christensen, R. I.; Gould, G. C. *Fuel Oil Desulfurization Symposium*; Japan Petroleum Institute: Tokyo, Japan, March 1970.
Weekman, V. W., Jr. *Proc. Int. Symp. Chem. React. Eng., 4th, April 6-8* **1976**, 615.

Received for review May 2, 1985
Revised manuscript received July 18, 1986
Accepted September 10, 1986

Kinetics of Liquefaction of Coal Catalyzed by Coal Minerals

Chandra P. P. Singh* and Norman L. Carr
Gulf Research & Development Company, Pittsburgh, Pennsylvania 15230

This work describes the development of a fundamental engineering understanding of the kinetics of coal liquefaction using a semiempirical kinetic model for SRC-II coal liquefaction (Singh et al., 1982a) and experimental data for liquefaction of several bituminous, subbituminous, and lignite coals in the presence of iron pyrite catalysts. The study establishes the applicability of one kinetic model to the liquefaction of widely different coals catalyzed by iron–sulfur catalysts in the coal minerals and/or iron pyrite catalysts. The source of the iron–sulfur catalyst has no effect, whereas H_2S has a strong inhibitive effect on the rate of hydrogenation reactions.

The term "coal liquefaction" is used to describe a variety of coal conversion processes whose major products range from a solid fuel (refined coal) to distillates of various boiling ranges (SRC-I: Anderson and Wright, 1975; Synthoil: Akhtar et al., 1974a,b. EDS: Epperly and Wade, 1981. H-Coal: Eccles and DeVaux, 1981. SRC-II: Freel et al., 1981. CCLP: Rosenthal et al., 1982). In each of these processes, organic matter in solid coal is converted to a liquid form by subjecting the coal to high temperatures (390–465 °C) and high hydrogen pressures (10–25 MPa). It appears that the same reactions occur in each of the processes, and the overall product from any process can be classified into the same categories of refined coal; light, middle, and heavy distillates or oil; asphaltene and preasphaltene; etc. However, distributions of products from various processes are vastly different. For example, the major product (over 50 wt % mf coal) from the SRC-I or Synthoil coal liquefaction process is a pyridine-soluble organic matter which boils above 482 °C, and only 10–15 wt % of the products are distillates, whereas in H-Coal or SRC-II, the distillates constitute a major part (30–45 wt % mf coal) of the overall product. These large variations in the product distributions result from significant differences in process conditions and the absence or use of different catalysts. These differences also reflect a significant change in importance of the various reactions.

For kinetic purposes, the above-referred processes need to be classified into two broad categories, viz., coal solvation and coal liquefaction. Coal solvation refers to the phase conversion of solid coal to a liquid under the reaction environment. The conversion involves physical processes as well as chemical reactions which are basically thermal

* Author to whom all correspondence should be addressed. Present address: Exxon Research & Engineering Company, Florham Park, NJ 07932.

0888-5885/87/2626-0501$01.50/0